J Intell Robot Syst (2017) 88:495–511
DOI 10.1007/s10846-016-0459-4

Tightly Bounding the Shortest Dubins Paths Through a Sequence of Points

Satyanarayana G. Manyam ·
Sivakumar Rathinam · **David Casbeer** ·
Eloy Garcia

Received: 6 September 2016 / Accepted: 15 December 2016 / Published online: 19 January 2017

Abstract This article addresses an important path planning problem for robots and Unmanned Aerial Vehicles (UAVs), which is to find the shortest path of bounded curvature passing through a given sequence of target points on a ground plane. Currently, no algorithm exists that can compute an optimal solution to this problem. Therefore, tight lower bounds are vital in determining the quality of any feasible solution to this problem. Novel tight lower bounding algorithms are presented in this article by relaxing some of the heading angle constraints at the target points. The proposed approach requires us to solve variants of an optimization problem called the Dubins interval problem between two points where the heading angles at the points are constrained to be within a specified interval. These variants are solved using tools from optimal control theory. Using these approaches, two lower bounding algorithms are presented and these bounds are then compared with existing results in the literature. Computational results are presented to corroborate the performance of the proposed algorithms; the average reduction in the difference between upper bounds and lower bounds is 80 % to 85 % with respect to the trivial Euclidean lower bounds.

Keywords Dubins paths · Curvature constrained paths · Lower bounds · Pontryagin's minimum principle · Dubins interval problem

1 Introduction

This article addresses the problem of finding a path of minimum length for a vehicle (car like robot) that needs to visit a prescribed sequence of points. The vehicle is modeled as a point robot, i.e., we ignore the dynamics of the vehicle and consider only its kinematic constraints. There are also no disturbances or obstacles in the environment. The path of the vehicle must satisfy a kinematic constraint, which limits the turning radius of the vehicle at all points along its path. This problem belongs to a well known class of motion constrained UAV (Unmanned Aerial Vehicle) routing problems that have received significant attention in the literature over the last decade [8, 13–16, 22, 25, 28, 30].

The problem of finding a shortest path for the vehicle to travel from a target at (x_1, y_1) with heading angle θ_1 to another target at (x_2, y_2) with heading angle θ_2 subject to the turning radius constraint of the vehicle has received significant attention in the literature over the last 50 years. L.E. Dubins [10] first solved this problem in 1957 and showed that

S. G. Manyam (✉) · D. Casbeer · E. Garcia
Control Science Center of Excellence, Air Force Research Laboratory, WPAFB, OH, USA
e-mail: msngupta@gmail.com

S. Rathinam
Department of Mechanical Engineering, Texas A & M University, College Station TX, USA

an optimal path must consist of at most three segments, where each of the segments must be either an arc of minimum turning radius (denoted as C) or a straight line (denoted as S). Specifically, Dubins [10] showed that the optimal path must either be of type CSC or CCC, or a degenerate form of these paths. An optimal path of the type CSC or CCC is typically referred to as a Dubins path in the literature. An alternate proof of this result by Dubins was developed by Boissonnat et al. in [3] using optimal control theory. There have also been extensions of these results for other vehicles; for example, in [29], Sussmann and Tang solved this shortest path problem for a vehicle that travels both forwards and backwards with the turning radius constraint. Variants of this problem in the presence of obstacles were also addressed in [1, 2, 4]. Shortest Dubins path through three points for the instances where the distance between any pair of targets is greater than 4ρ is solved in [27].

This article addresses an important generalization of the above problem where one aims to find a shortest path through the given sequence of target points subject to the turning radius constraint of the vehicle. We refer to this problem as the Generalized Dubins Path Problem (GDPP) in this article. This problem was first addressed by Lee et al.. in [11], where the authors present a 5.03-approximation algorithm. An α-approximation algorithm for a minimization problem is an algorithm that runs in polynomial time and finds a feasible solution whose cost is at most α times the optimal cost for the problem. This algorithm by Lee et al. [11] remains the only constant factor algorithm in the literature for the GDPP to date. For the special case when the Euclidean distance between any two adjacent points in the given sequence is at least equal to four times the minimum turning radius (ρ), Goaoc et al. [7] have recently shown that the optimal cost (or the length of the optimal solution) of the GDPP is convex in the heading angles at each target and that a gradient descent algorithm can find an optimum.

A generalization of the GDPP where a set of points is given but their sequence to visit is not given, and the vehicle has to return to its starting location after visiting all the points is the Dubins Traveling Salesman Problem (DTSP). DTSP has received considerable attention primarily due to its application in robotic and UAV path planning applications. Heuristics and approximation algorithms to solve the DTSP and its variants are presented in [6, 9, 12, 23, 25, 26, 30]; lower bounds to this problem are computed using Lagrangian relaxation in [19–21] and by relaxing the heading angle constraint at target points in [17].

Despite the numerous results available for finding feasible solutions for the GDPP (one can refer to [17] for a review of the methods available), there is currently no algorithm that can find an optimal solution to the GDPP. Therefore, it is of critical importance to develop algorithms or computationally efficient procedures that can provide tight lower bounds to the GDPP. The tight lower bounds act as proxies to the optimal costs, and as a result, the quality of a feasible solution can be computed with respect to the tight lower bounds.

A trivial lower bound can be obtained by simply removing the turning radius constraint of the vehicle; in this case, the lower bound is the sum of all the Euclidean distances between adjacent points in the given sequence. Computational results (you can be refer to the results section of this article) show that this trivial bound is quite conservative, and therefore, serves as a poor estimate of the optimal cost. Recently, a novel procedure was presented for developing tight lower bounds for the DTSP [17] by relaxing some of the angle constraints at each point. In this article, we generalize this procedure to develop other lower bounds for the GDPP. The following are the contributions of this article (a preliminary version of this paper without any of the proofs for the results appeared in [18]):

- At each prescribed point in a feasible path, the heading angle (incoming angle) for the section of the path that ends at the point should be the same as the heading angle (outgoing angle) at the beginning of the path segment that starts at the point. We relax this constraint at *some* points in the given sequence by allowing the incoming and the outgoing angles to be different but restrict their absolute difference to be within a given interval. We then pose the resulting relaxed problem as a shortest path problem. As any feasible solution to the GDPP is also a feasible solution to this relaxed problem, one obtains a lower bound. This procedure generalizes the result in [17].
- The computation of the lower bounds requires us to solve variants of an optimal control problem called the Dubins Interval Problem. Novel algorithms are provided to solve these variants using the Pontryagin's minimum principle [24].

– All the lower bound computation methods proposed are implemented and tested on several randomly generated instances to corroborate the performance of the proposed algorithms.

This article is organized as follows: the problem description is presented in Section 2. In Sections 3 and 5, we address the variants of the Dubins Interval Problem which arises while computing the lower bounds for the GDPP. The algorithms to compute lower bounds are presented in Section 5. The computational results are presented in Section 6, and finally conclusions are made in Section 7.

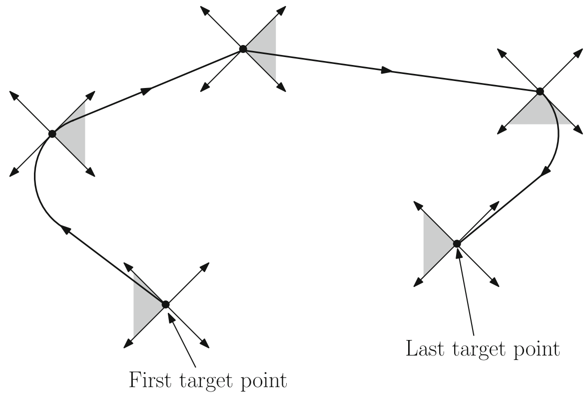

Fig. 1 Relaxed Dubins path

2 Problem Formulation

Let $T = \{t_1, t_2, \ldots, t_n\}$ be the prescribed sequence of n target points. An optimal path for the GDPP is a path of shortest length with bounded curvature that passes through all n target points. We aim to find a tight lower bound to the length of this optimal path by relaxing certain constraints at some of the points along the path. This optimal path is a concatenation of $n-1$ individual Dubins paths $\{d_{12}, d_{23}, \ldots d_{(n-1)n}\}$, where d_{ij} is a Dubins path from target i to j. For $i = 1 \ldots n$, let θ_i be the angle made by the tangent of the path at target t_i with respect to the x-axis. If the values of θ_i's are specified, one can construct each of the individual Dubins paths using the result in [10]. Therefore, the problem of solving the GDPP reduces to finding the heading angles (θ_i's) at each target point such that the resulting path is of minimal length.

Let $t_i, t_j,$ and t_k be the target points in a subsequence. Let θ_{ja} represent the final heading of the path d_{ij}, and θ_{jd} be the initial heading of the path d_{jk}. The path is feasible only if these two headings are equal, $\theta_{ja} = \theta_{jd} = \theta_j$. One can compute a lower bound to the GDPP by relaxing this angle constraint at the target points, i.e., at every target point, the incoming and outgoing angles are allowed to differ. This leads to a trivial lower bound, which is the sum of the Euclidean distances along the given sequence of points. We aim to find a tighter lower bound using the following relaxation: The incoming and outgoing headings may not be equal, but should be within a specified interval. A solution to the Dubins path problem with this relaxation is shown in Fig. 1.

Clearly, tighter lower bounds can be found by relaxing as few constraints as possible. We provide two algorithms to compute lower bounds, each with a different set of relaxations. In the first algorithm, we relax the heading angle constraint at every target point, and in the second we relax it only at alternate target points. The set of heading angles $[0, 2\pi)$ at a target point t_i is partitioned into a set of intervals $\mathcal{I}_i = \{[0, \phi_{i1}], [\phi_{i1}, \phi_{i2}], \ldots [\phi_{im-1}, \phi_{im} = 2\pi)\}$, such that $0 \le \phi_{i1} \le \phi_{i2} \ldots \phi_{im} = 2\pi$. This partitioning is done at every target point in the first relaxation criteria, and only at alternate points $\{t_1, t_3, \ldots\}$ in the second relaxation criteria. Computing the optimal solutions to these two relaxations requires us to find the shortest Dubins paths between two points where the departure angle and the arrival angle at the points belong to the specified intervals. Therefore, in the ensuing subsections, we formulate the two optimization problems that result from the two relaxations.

2.1 Relaxing the Heading Constraints at all the Points

Let (x_v, y_v) be the coordinates of target t_v in the global reference frame. Let θ_{va} denote the arrival (incoming) heading angle at any target t_v, and θ_{vd} denote the departure (outgoing) heading angle. In the first relaxation criteria, for every pair of successive target points (t_i, t_j) and intervals $I_i \in \mathcal{I}_i$, $I_j \in \mathcal{I}_j$, we need to solve the **two point Dubins interval problem**, i.e. find the shortest Dubins path d^*_{ij} between two points where the heading at those points belong to the specified intervals. In other words,

$$d^*_{ij}(I_i, I_j) = \min_{\theta_{id} \in I_i, \theta_{ja} \in I_j} d_{ij}(\theta_{id}, \theta_{ja}), \tag{1}$$

where, $d_{ij}(\theta_{id}, \theta_{ja})$ is the length of the Dubins path between t_i and t_j with headings θ_{id} at t_i and θ_{ja} at

t_j. A lower bound to the GDPP is given by the minimum of the summation $\sum_{i=1..n-1} d^*_{ii+1}(I_i, I_{i+1})$ over all possible intervals, I_i at all points $i = 1, \ldots, n$.

2.2 Relaxing the Heading Constraints at Alternate Points

Suppose t_i, t_j, t_k are target points to be visited in a sequence. Let the heading constraints be relaxed at targets t_i and t_k. Let $d_{ijk}(\theta_{id}, \theta_{ka})$ denote the length of the Dubins path from (x_i, y_i) to (x_k, y_k) with heading angles θ_{id} at t_i and θ_{ka} at t_k, such that the path passes through the point (x_j, y_j) with an unconstrained heading. We need to find the shortest Dubins path from t_i to t_k, such that the angle θ_{id} at t_i and θ_{ka} at t_k belongs to the given intervals I_i and I_k respectively. Let us denote this as

$$d^*_{ijk}(I_i, I_k) := \min_{\theta_{id} \in I_i,\, \theta_{ka} \in I_k} d_{ijk}(\theta_{id}, \theta_{ka}). \tag{2}$$

The problem stated in the above equation is referred to as the **three point Dubins interval problem**. The minimum of the summation of the length of the Dubins paths $\sum_{i=1,3..n-2} d^*_{i(i+1)(i+2)}(I_i, I_{i+2})$ over all the intervals at the points where the heading constraints are relaxed provides a lower bound to the GDPP.

In the following sections, we pose the two point and the three point Dubins Interval Problems as optimal control problems and solve using Pontryagin's minimum principle.

3 Two Point Dubins Interval Problem

Without any loss of generality, the objective of the two point Dubins interval problem is as follows:

$$\min_{\theta_1 \in I_1, \theta_2 \in I_2} d_{12}(\theta_1, \theta_2).$$

Let the intervals be denoted as $I_1 = [\theta_1^{min}, \theta_1^{max}]$ and $I_2 = [\theta_2^{min}, \theta_2^{max}]$. Also, let $I_1^o = (\theta_1^{min}, \theta_1^{max})$ and $I_2^o = (\theta_2^{min}, \theta_2^{max})$. We solved this problem recently using geometrical analysis [17]. In this article, we provide a simple algorithm for solving this problem using the Pontryagin′s minimum principle.

Theorem 1 *Suppose L and R represents the left (counter-clockwise) and the right (clockwise) circular arcs with radius equal to the minimum turning radius of the vehicle, and S represents a straight line. More specifically, L_ψ and R_ψ are the arcs subtended by angle ψ. The shortest path of bounded curvature between the two targets with the departure angle $\theta_1 \in I_1 = [\theta_1^{min}, \theta_1^{max}]$ at target 1 and the arrival angle $\theta_2 \in I_2 = [\theta_2^{min}, \theta_2^{max}]$ at target 2 must be one of the following candidate solutions or a degenerate form of these:*

Case 1: S or L_ψ or R_ψ or $L_\psi R_\psi$ or $R_\psi L_\psi$ with $\psi > \pi$.
Case 2: $\theta_1 = \theta_1^{max}$ and $\theta_2 = \theta_2^{max}$ and the path is LSR.
Case 3: $\theta_1 = \theta_1^{max}$ and $\theta_2 = \theta_2^{min}$ and the path is either LSL or $LR_\psi L$ with $\psi > \pi$.
Case 4: $\theta_1 = \theta_1^{min}$ and $\theta_2 = \theta_2^{min}$ and the path is RSL.
Case 5: $\theta_1 = \theta_1^{min}$ and $\theta_2 = \theta_2^{max}$ and the path is either RSR or $RL_\psi R$ with $\psi > \pi$.
Case 6: $\theta_1 = \theta_1^{max}$ and $\theta_2 \in I_2^o$ and the path is either LS or LR_ψ with $\psi > \pi$.
Case 7: $\theta_1 = \theta_1^{min}$ and $\theta_2 \in I_2^o$ and the path is either RS or RL_ψ with $\psi > \pi$.
Case 8: $\theta_1 \in I_1^o$ and $\theta_2 = \theta_2^{max}$ and the path is either SR or $L_\psi R$ with $\psi > \pi$.
Case 9: $\theta_1 \in I_1^o$ and $\theta_2 = \theta_2^{min}$ and the path is either SL or $R_\psi L$ with $\psi > \pi$.

Theorem 1 gives an algorithm for finding the optimal solution to the Dubins Interval Problem, namely, compare the paths for each case and choose the shortest candidate path. The following remark helps to solidify how this is possible.

Remark In cases 1 and 6–9, the departure and arrival angles are implicitly specified by the corresponding paths. For example in Case 1, if the path $L_\psi R_\psi$ (with $\psi > \pi$) exists between the two targets, where the length of segment L_ψ is equal to that of R_ψ, then the departure and arrival angles of the path are uniquely specified by the geometry. (We will discuss this fact in more detail in the proof of Theorem 1; refer to Fig. 2 for an example.) Similarly for Case 6, if $\theta_1 = \theta_1^{max}$, the arrival angle at target 2 is determined by the LS or LR_ψ paths. Feasibility can be determined by checking if the arrival angle at target 2 lies in the interval $\left[\theta_2^{min}, \theta_2^{max}\right]$.

3.1 The Minimum Principle

Denote the state of the vehicle at time t as $p(t) = (x(t), y(t), \theta(t))$ where $x(t)$, $y(t)$ and $\theta(t)$ represent

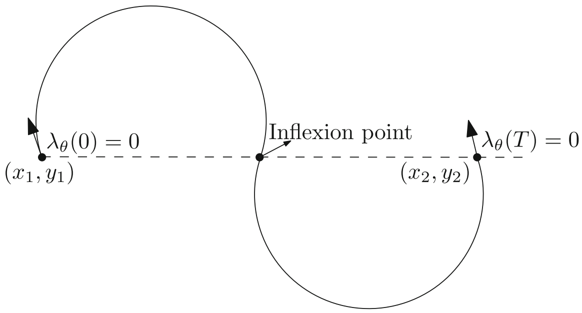

Fig. 2 A RL path with the boundary values of $\lambda_\theta(0) = \lambda_\theta(T) = 0$

the vehicle's x, y positions and heading respectively in the ground plane. The vehicle travels at constant speed v_o (> 0) with bounded control input, $u(t) \in \left[-\frac{v_o}{\rho}, \frac{v_o}{\rho}\right]$. The Dubins interval problem is formulated as an optimal control problem as follows:

$$\min_{u(t)\in\left[-\frac{v_o}{\rho}, \frac{v_o}{\rho}\right]} \int_0^T 1dt \tag{3}$$

subject to

$$\begin{aligned}\frac{dx}{dt} &= v_o \cos\theta,\\ \frac{dy}{dt} &= v_o \sin\theta,\\ \frac{d\theta}{dt} &= u,\end{aligned} \tag{4}$$

and the following boundary conditions:

$$x(0) = x_1, \quad x(T) = x_2, \tag{5}$$

$$y(0) = y_1, \quad y(T) = y_2, \tag{6}$$

$$\theta_1^{min} - \theta(0) \leq 0, \tag{7}$$

$$\theta(0) - \theta_1^{max} \leq 0, \tag{8}$$

$$\theta_2^{min} - \theta(T) \leq 0, \tag{9}$$

$$\theta(T) - \theta_2^{max} \leq 0. \tag{10}$$

Let the adjoint variables associated with $p(t) = (x(t), y(t), \theta(t))$ be denoted as $\Lambda(t) = (\lambda_x(t), \lambda_y(t), \lambda_\theta(t))$. The Hamiltonian associated with above system is defined as:

$$H(\Lambda, p, u) = 1 + v_o \cos\theta\lambda_x + v_o \sin\theta\lambda_y + u\lambda_\theta, \tag{11}$$

and the differential equations governing the adjoint variables are defined as:

$$\begin{aligned}\frac{d\lambda_x}{dt} &= 0,\\ \frac{d\lambda_y}{dt} &= 0,\\ \frac{d\lambda_\theta}{dt} &= v_o \sin\theta\lambda_x - v_o \cos\theta\lambda_y.\end{aligned} \tag{12}$$

Applying the fundamental theorem of Pontryagin [24] to the above problem, we obtain the following: If u^* is an optimal control to the Dubins interval problem, then there exists a non-zero adjoint vector $\Lambda(t)$ and $T > 0$ such that $p(t)$, $\Lambda(t)$ being the solution to the Eqs. 4 and 12 for $u(t) = u^*(t)$, the following conditions must be satisfied:

- $\forall t \in [0, T]$, $H(\Lambda, p, u^*) \equiv \min_{u\in\left[-\frac{v_o}{\rho}, \frac{v_o}{\rho}\right]} H(\Lambda, p, u)$.
- $\forall t \in [0, T]$, $H(\Lambda, p, u^*) \equiv 0$.
- Suppose $\alpha_1, \alpha_2, \beta_1, \beta_2$ are the Lagrange multipliers corresponding to the boundary conditions in Eqs. 7–10 respectively. Then, we have,

$$\alpha_1, \alpha_2, \beta_1, \beta_2 \geq 0, \tag{13}$$

$$\alpha_1(\theta_1^{min} - \theta(0)) = 0, \tag{14}$$

$$\alpha_2(\theta(0) - \theta_1^{max}) = 0, \tag{15}$$

$$\beta_1(\theta_2^{min} - \theta(T)) = 0, \tag{16}$$

$$\beta_2(\theta(T) - \theta_2^{max}) = 0, \tag{17}$$

$$\lambda_\theta(T) = \beta_2 - \beta_1, \tag{18}$$

$$\lambda_\theta(0) = \alpha_1 - \alpha_2. \tag{19}$$

Given a departure angle at target 1 and an arrival angle at target 2, the following facts are known for the basic Dubins problem in [3, 5]. These facts will be used in the proof of Theorem 1.

Fact 1 *Consider any point P on an optimal path which is either an inflexion point of the path (point joining two curved segments or a point joining a curved segment and a straight line) or any point on a straight line segment of the path. Suppose the vehicle crosses this point P at time $t \in [0, T]$. Then, $\lambda_\theta(t) = 0$.*

Fact 2 *All the points of an optimal path where* $\lambda_\theta(t) = 0$ *lie on the same straight line.*

Fact 3 *Consider any curved segment of an optimal path. Let the times* t_1, t_2 *be such that* $0 \leq t_1 < t_2 \leq T$*, the vehicle is located on the curved segment at times* t_1, t_2*, and* $\lambda_\theta(t_1) = \lambda_\theta(t_2) = 0$*. Then, the length of the curved segment between the times* t_1 *and* t_2 *must be greater than* $\pi\rho$*.*

Fact 4 *For any* $t \in [0, T]$*, the optimal control* $u^*(t) = -sign(\lambda_\theta(t))\frac{v_o}{\rho}$ *if* $\lambda_\theta(t) \neq 0$*.*

Fact 5 *If* $L_u R_v L_w$ *or* $R_u L_v R_w$ *is an optimal Dubins path, then* $\pi < v < 2\pi$*, and either* $0 \leq u < v - \pi$ *or* $0 \leq w < v - \pi$*.*

3.2 Proof of Theorem 1

The departure angle in any optimal solution must either be an interior point in I_1 or belong to one of the boundary values of I_1. Similarly, the arrival angle in any optimal solution must either be an interior point in I_2 or belong to one of the boundary values of I_2. The combination of choices for the departure and arrival angles coupled with the complementary slackness conditions in Eqs. 13–19 provides constraints for the values of $\lambda_\theta(0)$ and $\lambda_\theta(T)$. These constraints can then be used to find the candidate solutions for solving the Dubins interval problem. The following lemma first shows the relationship between the departure, arrival angles and the constraints on $\lambda_\theta(0)$ and $\lambda_\theta(T)$.

Lemma 1 *The constraints for the adjoint variable* λ_θ *at times* $t = 0$ *and* $t = T$ *corresponding to the departure and arrival angles are given in the table below:*

Case No.	*Conditions on the departure and arrival angles of any optimal path*	*Implied constraints on* $\lambda_\theta(0)$ *and* $\lambda_\theta(T)$
1	$\theta(0) \in I_1^o$, $\theta(T) \in I_2^o$	$\lambda_\theta(0) = 0, \lambda_\theta(T) = 0$
2	$\theta(0) = \theta_1^{max}$, $\theta(T) = \theta_2^{max}$	$\lambda_\theta(0) \leq 0, \lambda_\theta(T) \geq 0$
3	$\theta(0) = \theta_1^{max}$, $\theta(T) = \theta_2^{min}$	$\lambda_\theta(0) \leq 0, \lambda_\theta(T) \leq 0$
4	$\theta(0) = \theta_1^{min}$, $\theta(T) = \theta_2^{min}$	$\lambda_\theta(0) \geq 0, \lambda_\theta(T) \leq 0$
5	$\theta(0) = \theta_1^{min}$, $\theta(T) = \theta_2^{max}$	$\lambda_\theta(0) \geq 0, \lambda_\theta(T) \geq 0$
6	$\theta(0) = \theta_1^{max}$, $\theta(T) \in I_2^o$	$\lambda_\theta(0) \leq 0, \lambda_\theta(T) = 0$
7	$\theta(0) = \theta_1^{min}$, $\theta(T) \in I_2^o$	$\lambda_\theta(0) \geq 0, \lambda_\theta(T) = 0$
8	$\theta(0) \in I_1^o$, $\theta(T) = \theta_2^{max}$	$\lambda_\theta(0) = 0, \lambda_\theta(T) \geq 0$
9	$\theta(0) \in I_1^o$, $\theta(T) = \theta_2^{min}$	$\lambda_\theta(0) = 0, \lambda_\theta(T) \leq 0$

Proof Consider case 1, with constraints $\theta(0) \in I_1^o$, $\theta(T) \in I_2^o$ listed in the table. If $\theta(0) \in I_1^o$, then Eqs. 14 and 15 imply $\alpha_1 = 0$ and $\alpha_2 = 0$. Using Eq. 19, we obtain $\lambda_\theta(0) = \alpha_1 - \alpha_2 = 0$. Similarly, if $\theta(T) \in I_2^o$, then Eqs. 16 and 17 imply $\beta_1 = 0$ and $\beta_2 = 0$. Using Eq. 18, we obtain $\lambda_\theta(T) = \beta_2 - \beta_1 = 0$. The constraints for each case in the table can be verified using a similar procedure. □

We now use the constraints on $\lambda_\theta(0)$ and $\lambda_\theta(T)$ to infer the candidate solutions for the Dubins interval problem.

Lemma 2 *Let* $\lambda_\theta(0) = \lambda_\theta(T) = 0$*. Then the optimal path for the Dubins interval problem must be either* S *or* L_ψ *or* R_ψ *or* $L_\psi R_\psi$ *or* $R_\psi L_\psi$ *with* $\psi > \pi$*.*

Proof From Fact 2, a straight path S is a candidate optimal path as it satisfies the boundary conditions $\lambda_\theta(0) = \lambda_\theta(T) = 0$. From the family of paths with only one curved segment, i.e., R_ψ and L_ψ, Fact 3 states that only those of length greater than $\pi\rho$ can satisfy the boundary conditions $\lambda_\theta(0) = \lambda_\theta(T) = 0$. If an optimal path consists of exactly two curved segments, i.e., $L_\psi R_\psi$ or $R_\psi L_\psi$, then, from Fact 1 there are three points $((x_1, y_1), (x_2, y_2)$ and the inflection point) where $\lambda_\theta(t) = 0$ for $t \in [0, T]$. From Fact 2, these three points must lie on the same straight line. Therefore, the length of the first curved segment must be equal to the length of the second curved segment as shown in Fig. 2 (in this case, $\theta(0) = \theta(T)$), and from Fact 3 each of these curved segments must be longer than $\pi\rho$. In addition, paths containing three curved segments that satisfy the boundary conditions must have the length of each curved segment (between any two inflection points) greater than $\pi\rho$; however, from Fact 5, such a path cannot be optimal. Therefore, an optimal path may consist of either one or two curved segments with the length of each segment greater than $\pi\rho$. □

Note that a set of constraints, say $\lambda_\theta(0) \leq 0, \lambda_\theta(T) \geq 0$, can be satisfied if either $\lambda_\theta(0) = \lambda_\theta(T) = 0$ or $\lambda_\theta(0) < 0, \lambda_\theta(T) = 0$ or $\lambda_\theta(0) < 0, \lambda_\theta(T) > 0$ or $\lambda_\theta(0) = 0, \lambda_\theta(T) > 0$ is satisfied. The following lemma identifies all the candidate solutions for any combination of these constraints on $\lambda_\theta(0)$ and $\lambda_\theta(T)$.

Lemma 3 *Candidate solutions for the Dubins interval problem corresponding to the constraints on $\lambda_\theta(0)$ and $\lambda_\theta(T)$ are given in the table below:*

Constraints on $\lambda_\theta(0)$ and $\lambda_\theta(T)$	*Candidate solutions ($\psi > \pi$)*
$\lambda_\theta(0) = 0, \lambda_\theta(T) = 0$	$S, L_\psi, R_\psi, L_\psi R_\psi, R_\psi L_\psi$
$\lambda_\theta(0) < 0, \lambda_\theta(T) = 0$	LS, LR_ψ *with* $\psi > \pi$
$\lambda_\theta(0) < 0, \lambda_\theta(T) < 0$	$LSL, LR_\psi L$ *with* $\psi > \pi$
$\lambda_\theta(0) < 0, \lambda_\theta(T) > 0$	LSR
$\lambda_\theta(0) = 0, \lambda_\theta(T) < 0$	SL, RL_ψ *with* $\psi > \pi$
$\lambda_\theta(0) = 0, \lambda_\theta(T) > 0$	SR, LR_ψ *with* $\psi > \pi$
$\lambda_\theta(0) > 0, \lambda_\theta(T) = 0$	RS, RL_ψ *with* $\psi > \pi$
$\lambda_\theta(0) > 0, \lambda_\theta(T) < 0$	RSL
$\lambda_\theta(0) > 0, \lambda_\theta(T) > 0$	$RSR, RL_\psi R$ *with* $\psi > \pi$

Proof The candidate solutions corresponding to $\lambda_\theta(0) = \lambda_\theta(T) = 0$ has already been shown in Lemma 2.

Consider the next set of constraints $\lambda_\theta(0) < 0$ and $\lambda_\theta(T) = 0$. If $\lambda_\theta(0) < 0$, the first segment of the path must be L (Fact 4). LSR_ψ or LSL_ψ with $\psi > 0$ is not possible because this path would violate Fact 2 unless the length of the straight line is equal to 0. LRL is also not possible for the following reasons:

- It has been shown in [7] that LRL can lead to an optimal solution only if the Euclidean distance between the targets (d) is less than 4ρ. Therefore, without loss of generality, we can assume that $d < 4\rho$.
- There are three points where λ_θ is zero in such a path with $\lambda_\theta(T) = 0$ (refer to Fig. 3). This constraint on the points specifies the arrival angle, θ_2^*, at target 2.
- For a fixed departure angle θ_1, suppose $\mathfrak{D}(\theta_2)$ denote the length of the LRL path as a function of the arrival angle, θ_2, at target 2. In [17], it has been shown that $\frac{d\mathfrak{D}}{d\theta_2} = 0$ and $\frac{d^2\mathfrak{D}}{d\theta_2^2} < 0$ when $\theta_2 = \theta_2^*$ if $d < 4\rho$. Therefore, for a fixed departure angle, the length of the LRL path reaches a maximum when the arrival angle is θ_2^*. Hence, an LRL path with $\lambda_\theta(T) = 0$ cannot lead to an optimal solution. As a result, when $\lambda_\theta(0) < 0$ and $\lambda_\theta(T) = 0$, the possible candidates are LS or LR_ψ with $\psi > \pi$.

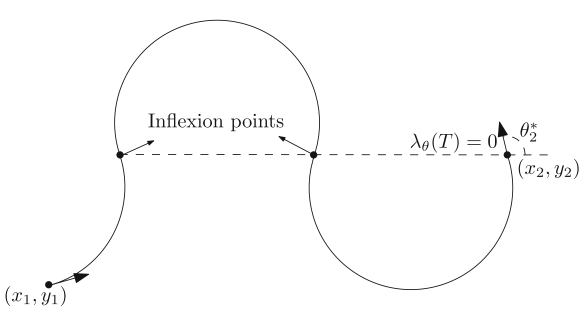

Fig. 3 A LRL path with $\lambda_\theta(T) = 0$

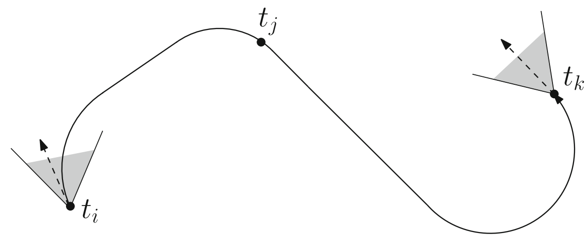

Fig. 4 Three point interval to interval Dubins path

Each of the remaining set of the constraints can be shown using a similar procedure. □

Theorem 1 follows by combining Lemmas 1 and 3.

4 Three Point Dubins Interval Problem

We will state the three point Dubins interval problem as the following: given the locations of three points (t_i, t_j, t_k), and two intervals $I_i, I_k \subset [0, 2\pi)$ at t_i and t_k respectively, find the shortest path such that (i) the path starts at t_i, passes through t_j and ends at t_k, (ii) the heading angles at t_i and t_k should lie within the given intervals $\theta_i \in I_i$, $\theta_k \in I_k$, (iii) the radius of curvature at any point along the path is at least equal to the minimum turning radius of the vehicle. Here, the intervals I_i and I_k are continuous and can be specified as $[\theta_i^{min}, \theta_i^{max}]$ and $[\theta_k^{min}, \theta_k^{max}]$ respectively. A sample solution to the three point Dubins interval problem is shown in Fig. 4.

The variables to be determined in this problem are the heading angles at the three points θ_i, θ_j and θ_k. If they are known, we can construct the shortest path using the Dubins result. We aim to solve this by breaking the path into two parts, the path from t_i to t_j and t_j to t_k. We discretize the angle[1]

[1]We do not obtain an optimal solution here for the three point interval problem using this discretization method. However, for any small $\epsilon > 0$, one can show that a careful discretization of the angles at the intermediate point leads to an ϵ-approximate solution.

at the intermediate point θ_j, i.e., pick a discrete set of angles $\Psi = \{\psi_1, \ldots \psi_p\}$, $\psi_i \in [0, 2\pi]$. For each angle $\psi_j \in \Psi$, we compute two paths (i) shortest path from t_i to t_j, with initial heading angle $\theta_i \in I_i$, and (ii) path from t_j to t_k with final heading angle $\theta_k \in I_k$. Let $\bar{d}_{ij}(I_i, \psi_j) = \min_{\theta_i \in I_i} d_{ij}(\theta_i, \psi_j)$ and $\bar{d}_{jk}(\psi_j, I_k) = \min_{\theta_k \in I_k} d_{jk}(\psi_j, \theta_k)$. We pick the heading angle at the intermediate point such that the sum of the length of the two paths is a minimum, $d^*_{ijk}(I_i, I_k) := \min_{\psi_j \in \Psi}[\bar{d}_{ij}(I_i, \psi_j) + \bar{d}_{jk}(\psi_j, I_k)]$.

Here, there are two sub-problems and we have to find the shortest Dubins paths in each. In the first sub-problem, the heading angle at the initial location is restricted to an interval of angles and the heading at the final location is given; where as in the second sub-problem, the heading at initial point is given and the heading at final point is restricted to an interval. Though they seem to be different problems, for a generic case considered herein, solving one of the problems is equivalent to solving the other. This result is explained in the following discussion.

Let t_i and t_j be two points with coordinates (x_i, y_i) and (x_j, y_j) respectively. Let θ_j be the given heading angle at t_j and $[\theta_i^{min}, \theta_i^{max}]$ be the interval of headings given at t_i.

Proposition 1 *The shortest Dubins path from t_i to t_j with a heading $\theta_i \in [\theta_i^{min}, \theta_i^{max}]$ at t_i and θ_j at t_j, and the shortest path from t_j to t_i with heading $\theta_j + \pi$ at t_j and $\theta_i + \pi \in [\theta_i^{min} + \pi, \theta_i^{max} + \pi]$ at t_i are isometric.*

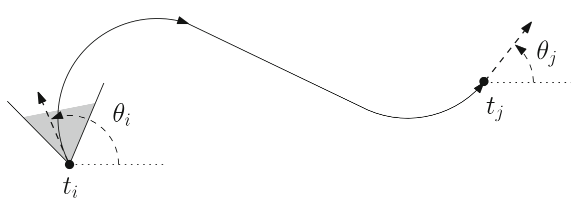

(a) Dubins path with heading at the initial point restricted to an interval and heading at final point given

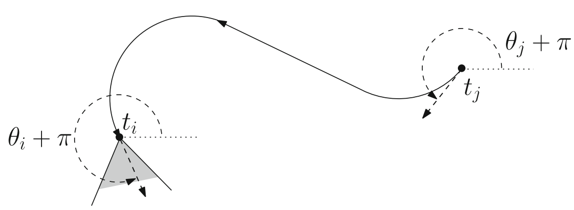

(b) Dubins path with heading at the initial point given and heading at final point restricted to an interval

Fig. 5 Equivalent Dubins paths between two points

Proof From symmetry and Fig. 5, those two paths are equivalent. □

Without any loss of generality, the sub-problem here can be stated as follows: given two points t_1, t_2, the heading angle θ_1 at t_1 and an interval I_2 at t_2, find a shortest Dubins path from t_1 to t_2 such that the arrival angle of the Dubins path lies in the given interval. This problem in general can be stated as follows:

$$\min_{u(t) \in \left[-\frac{v_o}{\rho}, \frac{v_o}{\rho}\right]} \int_0^T 1 dt \tag{20}$$

subject to

$$\dot{x} = v_o \cos\theta, \tag{21}$$
$$\dot{y} = v_o \sin\theta, \tag{22}$$
$$\dot{\theta} = u, \tag{23}$$
$$x(0) = x_1, \qquad x(T) = x_2, \tag{24}$$
$$y(0) = y_1, \qquad y(T) = y_2, \tag{25}$$
$$\theta(0) = \theta_1, \tag{26}$$
$$\theta_2^{min} - \theta(T) \leq 0, \tag{27}$$
$$\theta(T) - \theta_2^{max} \leq 0. \tag{28}$$

This problem is a special case of the two point Dubins interval problem where the heading angle at the initial point is given. The algorithm for solving this special case is stated in the following corollary. This corollary can be shown using the proof of Theorem 1.

Corollary 1 *Any shortest path which is C^1 and piecewise C^2 of bounded curvature between two points with the departure angle θ_1 at point t_1 and the arrival angle $\theta_2 \in I_2 = [\theta_2^{min}, \theta_2^{max}]$ at point t_2 must be one of the following or a degenerate form of these:*

Case 1: The path is either LS or RS or LR_ψ or RL_ψ with $\psi > \pi$.

Case 2: $\theta_2 = \theta_2^{max}$ and the path is either LSR or RSR or $RL_\psi R$ with $\psi > \pi$.

Case 3: $\theta_2 = \theta_2^{min}$ and the path is either RSL or LSL or $LR_\psi L$ with $\psi > \pi$.

5 Lower Bounds Computation

In this section, we discuss the implementation details of the lower bounding algorithms. In addition, we also discuss an existing lower bound in the literature that can be obtained using the approximation algorithm in [11]. All these lower bounds are then tested on several instances to corroborate their performance.

5.1 Lower Bounds from Relaxations

To implement the relaxations, we divide the possible headings $[0, 2\pi)$ at target points into a set of p intervals; this is done at every point in the first relaxation, referred to as *Relax-2-point*, and at alternate points in the second relaxation, referred to as *Relax-3-point*. We chose the intervals at each point to be of same size (uniform intervals), and the same intervals are chosen at all the relaxed points. At each relaxed point t_i, the set of intervals would be $\mathcal{I}_i = \{[0 = \phi_{i0}, \phi_{i1}], [\phi_{i1}, \phi_{i2}], \dots [\phi_{i(p-1)}, \phi_{ip} = 2\pi]\}$. The size of the intervals is $\phi_{i1} - \phi_{i0} = \phi_{i2} - \phi_{i1} = \dots \phi_{ip} - \phi_{i(p-1)} = \phi_d$(constant), $\forall i = 1 \dots n$. Now, we compute the lower bound to the Dubins path problem by constructing a graph G, and solving a corresponding shortest path problem on G. The algorithms *Relax-2-point* and *Relax-3-point* present the construction of graphs based on the two different relaxations, and a lower bound to the GDPP is computed by finding the length of the shortest path on these graphs.

Algorithm 1 Relax-2-point

1. Divide the set of heading angles at each point t_i and create the set of intervals $\mathcal{I}_i = \{I_{i1}, \dots I_{ip}\}$ for $i = 1 \dots n$.
2. Construct a graph G^1 as the following: add a node to G^1 corresponding to each interval $I_{ik} \in \mathcal{I}_i$, $\forall i = 1 \dots n$, $k = 1 \dots p$; add an edge between two nodes corresponding to any two interval I_{im}, I_{i+1n}, if they belong to interval sets $\mathcal{I}_i$ and $\mathcal{I}_{i+1}$ at successive points; set the weight of the edge to be the distance of the shortest Dubins path between the interval I_{im} to I_{i+1n}.
3. Add an auxiliary node v_0, and add edges from v_0 to every node corresponding to all of the intervals in the set $\mathcal{I}_1$. Set the weight of all these edges to be zero.
4. Add an auxiliary node v_{n+1}, and add edges from all the nodes corresponding to the intervals in $\mathcal{I}_n$ to v_{n+1}; set the weight of these edges to be zero.
5. Compute the shortest path on G^1 from v_0 to v_{n+1} using the Dijkstra's algorithm.

Algorithm 2 Relax-3-point

1. Divide the heading angles at alternate points into set of intervals $\mathcal{I}_i = \{I_{i1}, \dots I_{ip}\}$ for $i = 1, 3, \dots (n-1)/n$, as shown in Fig. 6a. If the number of points are odd, then the heading angles at the last point t_n are discretized; if they are even, the angles at point t_{n-1} are discretized.
2. Construct a graph G^2 as follows: add a node to G^2 corresponding to each interval $I_{ik} \in \mathcal{I}_i$, $i = 1, 3 \dots$, $k = 1 \dots p$; add an edge between any two nodes corresponding to interval $I_{im}, I_{(i+2)n}$, if they belong to successive interval sets $\mathcal{I}_i$ and $\mathcal{I}_{i+2}$; set the weight of the edge to be the distance of the Dubins path between the interval I_{im} to $I_{(i+2)n}$ which passes through the point t_{i+1} (computed using the procedure presented in Section 3).
3. Add an auxiliary node v_0, and add edges connecting v_0 to all the nodes corresponding to the intervals $I_{1k} \in \mathcal{I}_1$. Set the weights of all these edges to be zero.
4. If the number of points are odd, add an auxiliary node v_{n+1}, and add edges connecting all the nodes corresponding to the intervals in $\mathcal{I}_n$ to v_{n+1}; set the weights of these edges to be zero.

   If the number of points are even, then add a node (v_n) corresponding to the point t_n; add edges from each node corresponding to all the intervals in $\mathcal{I}_{n-1}$ to v_n. Set the weight of these edges to be the length of the Dubins paths from the corresponding interval $I_{(n-1)k} \in \mathcal{I}_{n-1}$ to the point t_n.
5. Compute the shortest path on G^2 from v_0 to v_n (or v_{n+1}) using the Dijkstra's algorithm.

5.2 Computation of a Lower Bound using Lee et al.'s Approximation Algorithm [11]

In this section, we briefly outline a lower bound we compute from the approximation algorithm presented in [11]. The algorithm in [11] first identifies all the subsequences of points where the distance between any two adjacent points in each subsequence is at most equal to twice the minimum radius of the vehicle. Given such a subsequence, the algorithm further decomposes this subsequence into smaller

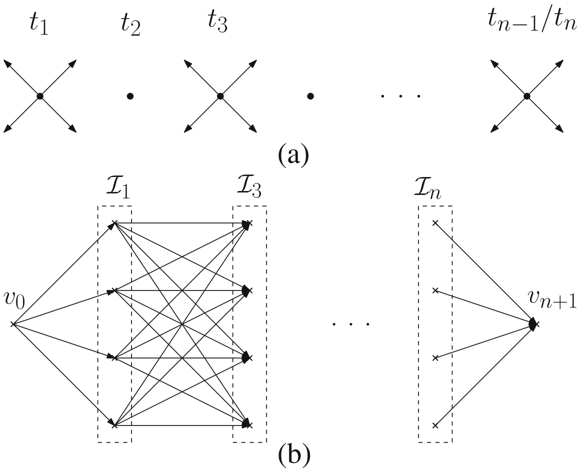

Fig. 6 Graph construction to compute lower bound

subsequences, say $S_1, S_2, \cdots, S_r$ where one of the following properties is guaranteed for each S_i:

1. There is a *direct* path (refer to Fig.7) for the vehicle through all the points in S_i, or,
2. There is at least one pair of adjacent points (u, v) in S_i where the length of any feasible Dubins path for the GDPP from u to v is at least equal to $\pi\rho$ where ρ is the minimum turning radius of the vehicle.

Therefore, using this approximation algorithm, one can obtain a lower bound for the GDPP in the following way: Without loss of generality, suppose

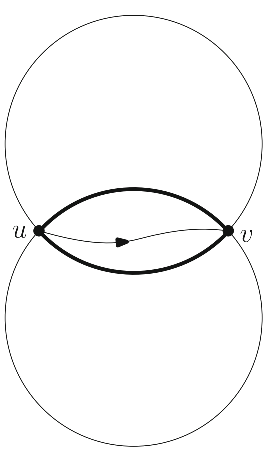

Fig. 7 A direct path between two points u and v that are at most 2ρ apart is a path that lies in the *shaded* region connecting the two target points. Here, the radius of the circles that pass through the target points is equal to ρ. A feasible path P through a sequence of points is referred to as a direct path if the part of P that lies between any two adjacent points in P is a direct path

$S_1^*, S_2^*, \cdots, S_l^*$ denote the subsequences where the distances between any two adjacent points in the subsequences is at most equal to 2ρ and there is at least one adjacent pair of points in each subsequence where the property 2 above is satisfied. The following is a then a lower bound for the GDPP:

$$\sum_{i=1}^{n-1} d(t_i, t_{i+1}) + \sum_{i=1}^{l} \min_{(u,v)\in S_i^*} (\pi\rho - d(u, v))$$

where $d(u, v)$ denotes the Euclidean distance between any adjacent target points u and v.

6 Computational Results

The computational experiments are run for two different problem sizes, instances with 11 and 21 target points. We generated 25 instances for each problem size. The coordinates of the points are generated from an uniform distribution in an area of 1000×1000 units. The turning radius of the vehicle is chosen to be 100 units. The sequence of the points is chosen by solving a Hamiltonian path problem on the generated points. All the algorithms are coded in MATLAB and the computations are run on Dell Precision Workstation (Intel Xeon Processor @2.53 GHz, 12 GB RAM).

Figure 8 compares the lower bounds computed using the two algorithms *Relax-3-point* and *Relax-2-point*. The lower bound computed using the result from [11] and the trivial Euclidean lower bounds are shown too. Clearly, relaxing at alternate points must produce tighter lower bounds compared to relaxing at all the points. This fact is corroborated by the lower bounds here. Also, the lower bounds computed using the proposed algorithms presented in this article are tighter than the bounds computed using the algorithm in [11]. Along with the lower bounds, the upper bounds for the instances are shown in this figure. The upper bounds are computed using the following method:

Upper Bound Computation At each point, a discrete set Φ_d of headings are chosen by uniformly sampling from the set $[0, 2\pi]$, $|\Phi_d| = 128$. A graph is constructed (similar to the graph in the algorithm *Relax-2-point*) where each heading at each point corresponds to a node; nodes corresponding to successive target points are connected with edges with weight equal to the Dubins distance between those points

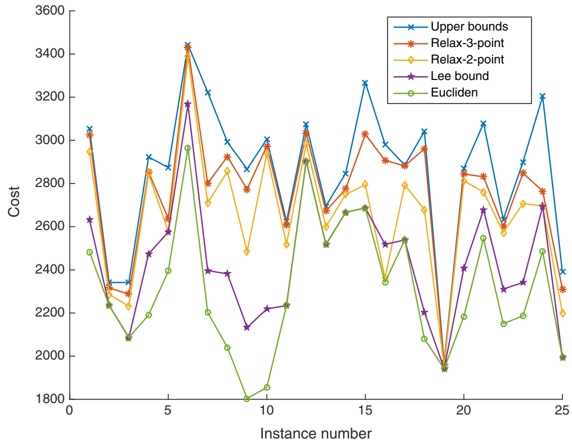

(a) Instances with 11 target points

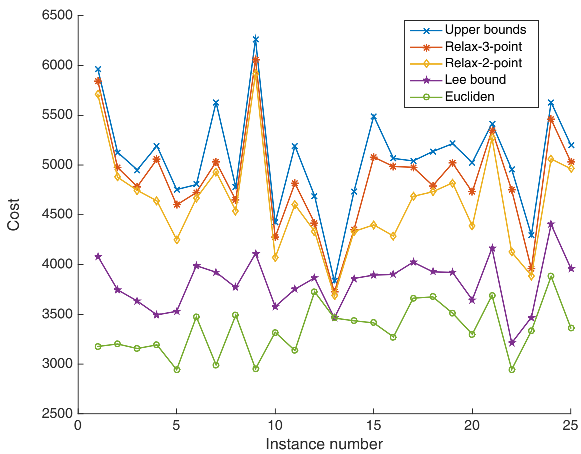

(b) Instances with 21 target points

Fig. 8 Comparison of the lower bounds computed using the three algorithms. The plots include the upper bounds and trivial lower bounds (Euclidean length)

with the corresponding headings. Two auxiliary nodes (v_0, v_{n+1}) are added to the graph, node v_0 is connected to each of the nodes that corresponds to the first target point with zero cost edges. Node v_{n+1} is connected to all the nodes correspond to the last target point with zero cost edges. The shortest path on this graph from v_0 to v_{n+1} gives a feasible path for the GDPP. The length of this path is an upper bound to the optimal solution to the GDPP.

We refer to the difference between upper bound and lower bound as gap, and if the new lower bound computed is greater than Euclidean lower bound, then the gap is reduced. The average gap reduction using $Relax-2-point$ algorithm is 58 % and 73 % for instances with 11 and 21 targets respectively, and it is 80 % and 85 % with $Relax-3-point$ algorithm. These two bounds outperformed the Lee's bound where the average gap reduction is 20 % and 31 % for the instances with 11 and 21 targets. Tables 1 and 2 lists all the lower bounds for 50 random instances computed along with the upper bounds and the Euclidean lower bound.

Figure 9 shows the lower bounds computed using the algorithm *Relax-3-point* and the trivial lower

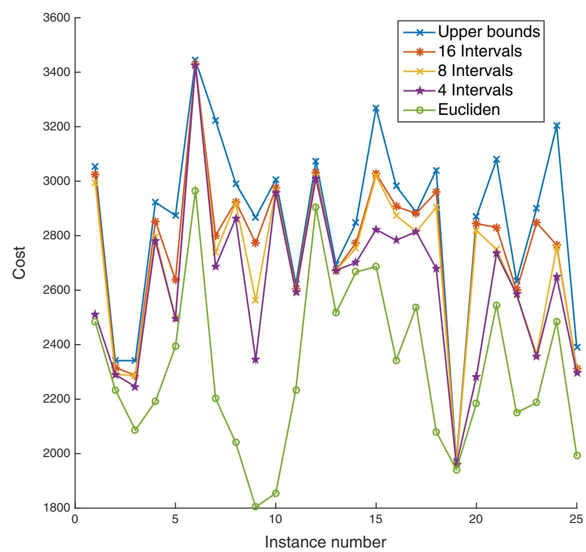

(a) Instances with 11 target points

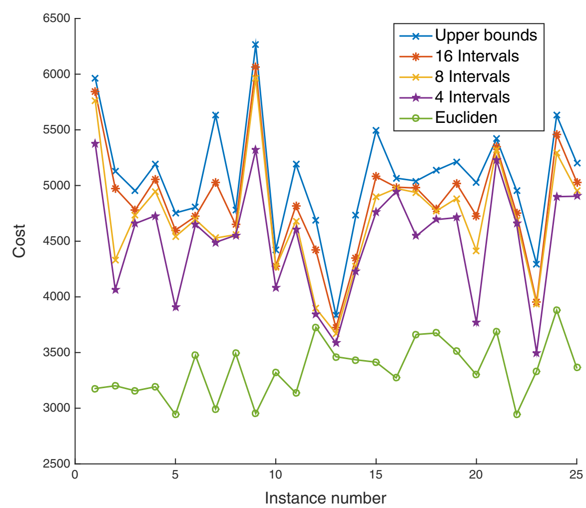

(b) Instances with 21 target points

Fig. 9 Lower bounds computed using interval discretization at alternate points (*Relax-3-point*) with 4, 8, and 16 intervals at each relaxed point bound (Euclidean length) for the 25 instances. It shows the bounds computed using three different sets of discretization, 4, 8 and 16 intervals respectively. One can observe that as the discretization level increases, the lower bounds increases for every instance, which is as expected. It indicates that, as the intervals at target points are narrowed down to a smaller size, the algorithm produces tighter lower bounds, and will eventually converge to an optimal solution of the problem.

The paths generated using the solution to the relaxed GDPP for one of the the instances (#8) with 21 targets is shown in Fig. 10. The feasible path (upper bound) for this instance is shown using dashed lines and curves. At each relaxed point, the headings are divided into 16 uniform intervals, i.e., each interval size is $\pi/4$. One can observe that the heading angles are discontinuous at some of the points in the relaxed path. But the difference between the incoming and outgoing headings is less than $\pi/4$ at every point.

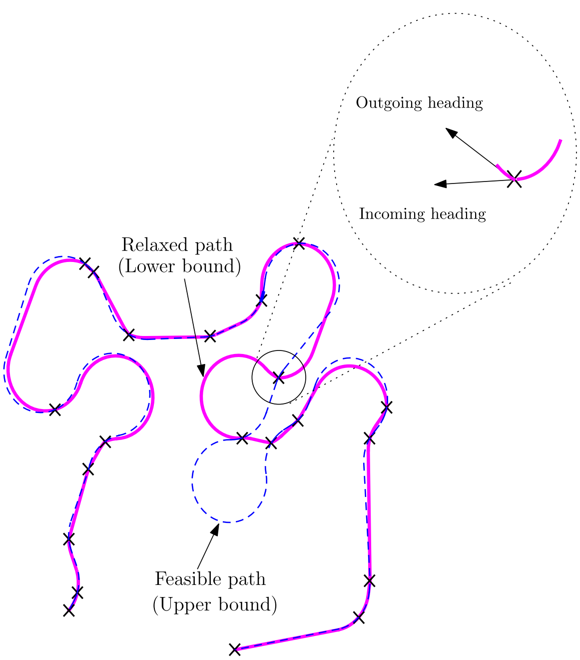

Fig. 10 Feasible Dubins path and the relaxed path computed using $Relax - 3 - point$ algorithm with 16 intervals for the instance # 8 with 21 targets. Length of the feasible path (upper bound) is 4776.70 units and the length of the relaxed path (lower bound) is 4558.94 units

7 Conclusions

We presented algorithms to compute tight lower bounds to the problem of finding a shortest path of bounded curvature passing through a sequence of points. We presented two different relaxations; the optimal solutions of these relaxed problems are lower bounds to the original shortest path problem. We presented the methods to solve the sub-problems that arise, the two point and three point Dubins interval problems. We characterized the optimal solutions for these sub-problems using Pontryagin's minimum principle and could find the optimal paths. We also computed lower bounds using the 5.03-approximation algorithm in [11]. We tested all the bounds on several instances generated from an uniform distribution. The lower bounds computed using the proposed relaxations outperformed the bounds from 5.03-approximation algorithm, and are with in 10 % of the best known upper bounds for every instance. The average reduction in the gap between upper bounds and lower bounds is 80 % to 85 % when compared with Euclidean lower bound. A scope for improving this result lies in characterizing the Dubins paths that passes through three points using optimal control theory. This may lead to solving the sub-problem with lesser computational effort.

Appendix

The algorithms are tested on 50 randomly generated instances, and the computational results are presented in Tables 1 and 2. Also listed are the Euclidean lower bound and the upper bound, which is the cost of the best feasible solution. In Table 1, columns four, six and eight refers to the lower bounds computed using the algorithms $Relax-2-point$, $Relax-3-point$ and Lee's bound respectively. The **percent reduction of gap** with the lower bounds computed using the algorithms in this article are presented in the columns five, seven and nine. Table 2 presents the lower bounds computed and the reduction in gap for the 50 instances with 4, 8 and 16 intervals. For each instance, the lower bounds are improved with higher set of intervals as expected.

Table 1 Lower bounds computed using *Relax-2-point*, *Relax-3-point* and Lee's algorithms

Instance #	Euc. Lower Bound	Upper Bound	Relax 2-point	% Gap reduced	Relax 3-point	% Gap reduced	Lee's bound	% Gap reduced
Instances with 11 targets								
1	2482.91	3054.54	2948.17	81.39	3025.26	94.88	2632.09	26.10
2	2234.72	2341.23	2286.44	48.56	2316.04	76.35	2234.72	0
3	2086.3	2341.48	2231.79	57.01	2287.42	78.81	2086.30	0
4	2190.71	2922.79	2843.98	89.24	2853.40	90.52	2516.73	44.53
5	2393.26	2874.08	2577.84	38.39	2638.09	50.92	2575.81	37.97
6	2965.83	3442.61	3389.18	88.79	3429.49	97.25	3217.69	52.83
7	2202.62	3223.30	2710.62	49.77	2800.84	58.61	2413.90	20.70
8	2041.05	2992.21	2855.50	85.63	2924.92	92.92	2400.95	37.84
9	1803.86	2866.75	2484.67	64.05	2773.29	91.21	2141.65	31.78
10	1854.99	3005.47	2938.74	94.20	2973.76	97.24	2218.56	31.60
11	2234.73	2623.67	2518.75	73.02	2606.08	95.48	2234.73	0
12	2904.19	3073.93	2982.45	46.11	3033.32	76.08	2904.19	0
13	2516.84	2695.46	2599.14	46.08	2673.14	87.50	2516.84	0
14	2666.72	2847.26	2749.23	45.70	2774.00	59.42	2666.72	0
15	2686.43	3267.91	2794.40	18.57	3027.84	58.71	2686.43	0
16	2342.79	2981.94	2362.05	3.01	2907.05	88.28	2625.54	44.24
17	2538.41	2885.30	2793.89	73.65	2881.65	98.95	2538.41	0
18	2080.38	3041.03	2677.54	62.16	2960.23	91.59	2203.57	12.82
19	1941.58	1969.27	1951.21	34.78	1962.15	74.29	1941.58	0
20	2183.65	2869.49	2812.71	91.72	2843.61	96.23	2459.79	40.26
21	2545.02	3078.77	2760.88	40.44	2831.14	53.60	2678.56	25.02
22	2150.09	2633.66	2573.09	87.47	2598.98	92.83	2353.77	42.12
23	2186.93	2900.10	2707.03	72.93	2847.86	92.67	2458.33	38.06
24	2484.38	3203.49	2696.45	29.49	2765.22	39.05	2758.72	38.15
25	1992.48	2389.46	2200.69	52.45	2311.19	80.28	1992.48	0
Mean	2308.43	2861.00	2657.85	58.98	2761.83	80.54	2458.32	20.96
Instances with 21 targets								
1	3176.85	5965.30	5710.84	90.87	5846.2	95.73	4347.93	42.00
2	3201.71	5128.62	4877.7	86.98	4976.12	92.09	3795.43	30.81
3	3156.31	4951.59	4745.69	88.53	4782.01	90.55	3696.56	30.09
4	3193.02	5192.39	4639.65	72.35	5057.23	93.24	3647.23	22.72
5	2943.22	4753.66	4250.63	72.22	4599.19	91.47	3808.14	47.77
6	3474.45	4803.15	4666.14	89.69	4723.36	93.99	4008.28	40.18
7	2992.02	5629.66	4932.5	73.57	5031.10	77.31	4242.06	47.39
8	3491.52	4776.70	4541.73	81.72	4647.55	89.95	3885.89	30.69
9	2952.22	6263.88	5916.44	89.51	6060.13	93.85	4283.14	40.19
10	3320.01	4421.13	4070.00	68.11	4274.83	86.71	3576.85	23.33
11	3135.85	5192.22	4601.59	71.28	4816.01	81.70	3837.87	34.14
12	3726.84	4688.89	4332.77	62.98	4417.83	71.82	3865.82	14.45
13	3462.21	3833.65	3686.11	60.28	3723.07	70.23	3462.21	0
14	3434.74	4735.93	4332.31	68.98	4351.59	70.46	4042.95	46.74
15	3413.84	5492.33	4398.76	47.39	5079.12	80.12	4143.42	35.10

Table 1 (continued)

Instance #	Euc. Lower Bound	Upper Bound	Relax 2-point	% Gap reduced	Relax 3-point	% Gap reduced	Lee's bound	% Gap reduced
16	3272.82	5066.38	4286.49	56.52	4985.26	95.48	3942.38	37.33
17	3661.97	5041.10	4684.95	74.18	4977.33	95.38	4179.77	37.55
18	3675.17	5136.21	4731.54	72.30	4792.75	76.49	3932.01	17.58
19	3510.94	5214.60	4820.96	76.89	5019.40	88.54	3929.69	24.58
20	3299.57	5025.79	4387.82	63.04	4728.90	82.80	3825.10	30.44
21	3690.13	5417.85	5270.79	91.49	5350.11	96.08	4358.47	38.68
22	2945.99	4957.04	4123.81	58.57	4747.96	89.60	3417.16	23.43
23	3333.08	4295.88	3889.27	57.77	3955.46	64.64	3535.23	2.001
24	3880.68	5629.64	5061.00	67.49	5459.34	90.26	4409.45	30.23
25	3363.16	5201.39	4962.71	87.02	5031.85	90.78	3962.06	32.58
Mean	3348.33	5072.59	4636.88	73.18	4857.34	85.97	3925.40	31.16

Table 2 Lower bounds computed using *Relax-3-point* for instances using 4, 8 and 16 intervals

Instance #	Euc. Lower Bound	Upper Bound	4 Intervals	% Gap reduced	8 Intervals	% Gap reduced	16 Intervals	% Gap reduced
Instances with 11 targets								
1	2482.91	3054.54	2512.25	5.13	2992.65	89.17	3025.26	94.88
2	2234.72	2341.23	2290.38	52.26	2291.14	52.97	2316.04	76.35
3	2086.30	2341.48	2245.65	62.45	2286.00	78.26	2287.42	78.81
4	2190.71	2922.79	2781.28	80.67	2796.25	82.72	2853.40	90.52
5	2393.26	2874.08	2496.20	21.41	2498.51	21.89	2638.09	50.92
6	2965.83	3442.61	3425.73	96.46	3425.95	96.51	3429.49	97.25
7	2202.62	3223.30	2686.40	47.40	2739.21	52.57	2800.84	58.61
8	2041.05	2992.21	2862.93	86.41	2918.99	92.30	2924.92	92.93
9	1803.86	2866.75	2344.91	50.90	2564.55	71.57	2773.29	91.21
10	1854.99	3005.47	2955.83	95.69	2965.14	96.49	2973.76	97.24
11	2234.73	2623.67	2592.48	91.98	2593.88	92.34	2606.08	95.48
12	2904.19	3073.93	3009.97	62.32	3015.52	65.59	3033.32	76.08
13	2516.84	2695.46	2672.43	87.11	2672.48	87.13	2673.14	87.50
14	2666.72	2847.26	2701.65	19.35	2754.26	48.49	2774.00	59.42
15	2686.43	3267.91	2822.52	23.40	3019.85	57.34	3027.84	58.71
16	2342.79	2981.94	2783.21	68.91	2873.93	83.10	2907.05	88.28
17	2538.41	2885.30	2814.46	79.58	2815.35	79.84	2881.65	98.95
18	2080.38	3041.03	2678.87	62.30	2903.48	85.68	2960.23	91.59
19	1941.58	1969.27	1958.83	62.30	1959.26	63.85	1962.15	74.29
20	2183.65	2869.49	2283.28	14.53	2819.94	92.78	2843.61	96.23
21	2545.02	3078.77	2734.27	35.46	2748.95	38.21	2831.14	53.61
22	2150.09	2633.66	2584.87	89.91	2586.20	90.19	2598.98	92.83
23	2186.93	2900.10	2355.40	23.62	2365.85	25.09	2847.86	92.67
24	2484.38	3203.49	2649.08	22.90	2758.14	38.07	2765.22	39.05
25	1992.48	2389.46	2295.33	76.29	2308.05	79.49	2311.19	80.28
Mean	2308.43	2861.01	2621.53	56.75	2706.94	70.47	2761.84	80.55

Table 2 (continued)

Instance #	Euc. Lower Bound	Upper Bound	4 Intervals	% Gap reduced	8 Intervals	% Gap reduced	16 Intervals	% Gap reduced
Instances with 21 targets								
1	3176.85	5965.30	5376.44	78.88	5765.63	92.84	5846.20	95.73
2	3201.71	5128.62	4065.34	44.82	4333.39	58.73	4976.12	92.09
3	3156.31	4951.59	4658.64	83.68	4733.58	87.86	4782.01	90.55
4	3193.02	5192.39	4729.21	76.83	4946.53	87.70	5057.23	93.24
5	2943.22	4753.66	3903.81	53.06	4541.41	88.28	4599.19	91.47
6	3474.45	4803.15	4650.99	88.55	4694.27	91.81	4723.36	93.99
7	2992.02	5629.66	4489.63	56.78	4528.33	58.25	5031.10	77.31
8	3491.52	4776.70	4553.20	82.61	4558.94	83.06	4647.55	89.95
9	2952.22	6263.88	5318.78	71.46	5964.41	90.96	6060.13	93.85
10	3320.01	4421.13	4086.15	69.58	4265.57	85.87	4274.83	86.71
11	3135.85	5192.22	4603.04	71.35	4679.30	75.06	4816.01	81.71
12	3726.84	4688.89	3846.78	12.47	3897.32	17.72	4417.83	71.82
13	3462.21	3833.65	3582.92	32.50	3671.35	56.31	3723.07	70.23
14	3434.74	4735.93	4232.05	61.28	4279.25	64.90	4351.59	70.46
15	3413.84	5492.33	4761.48	64.84	4897.17	71.37	5079.12	80.12
16	3272.82	5066.38	4944.73	93.22	4973.91	94.84	4985.26	95.48
17	3661.97	5041.10	4546.18	64.11	4936.85	92.44	4977.33	95.38
18	3675.17	5136.21	4693.93	69.73	4770.93	75.00	4792.75	76.49
19	3510.94	5214.60	4711.57	70.47	4883.20	80.55	5019.40	88.54
20	3299.57	5025.79	3768.18	27.15	4414.60	64.59	4728.90	82.80
21	3690.13	5417.85	5226.97	88.95	5324.62	94.60	5350.11	96.08
22	2945.99	4957.04	4657.52	85.11	4684.63	86.45	4747.96	89.60
23	3333.08	4295.88	3499.51	17.29	3936.95	62.72	3955.46	64.64
24	3880.68	5629.64	4899.87	58.27	5289.38	80.55	5459.34	90.26
25	3363.16	5201.39	4903.79	83.81	4950.62	86.36	5031.85	90.78
Mean	3348.33	5072.60	4508.43	64.27	4716.89	77.15	4857.35	85.97

References

1. Agarwal, P.K., Raghavan, P., Tamaki, H.: Motion planning for a steering-constrained robot through moderate obstacles. In: Symposium on Theory of Computing, pp. 343–352. ACM (1995)
2. Agarwal, P.K., Wang, H.: Approximation algorithms for curvature-constrained shortest paths. SIAM J. Comput. **30**(6), 1739–1772 (2001)
3. Boissonnat, J.D., Cérézo, A., Leblond, J.: Shortest paths of bounded curvature in the plane. J. Intell. Robot. Syst. **11**(1-2), 5–20 (1994). doi:10.1007/BF01258291
4. Boissonnat, J.D., Lazard, S.: A polynomial-time algorithm for computing shortest paths of bounded curvature amidst moderate obstacles. Int. J. Comput. Geom. Appl. **13**(03), 189–229 (2003)
5. Bui, X.N., Boissonnat, J.D., Soueres, P., Laumond, J.P.: Shortest path synthesis for Dubins non-holonomic robot. In: IEEE International Conference on Robotics and Automation, 1994. Proceedings, 1994, vol. 1, pp. 2–7 (1994). doi:10.1109/ROBOT.1994.351019
6. Epstein, C., Cohen, I., Shima, T.: On the discretized dubins traveling salesman problem. Technical Report (2014)
7. Goaoc, X., Kim, H.S., Lazard, S.: Bounded-curvature shortest paths through a sequence of points using convex optimization. SIAM J. Comput. **42**(2), 662–684 (2013)
8. Kenefic, R.J.: Finding good dubins tours for uavs using particle swarm optimization. J. Aerosp. Comput. Inf. Commun. **5**(2), 47–56 (2008)
9. Le Ny, J., Feron, E., Frazzoli, E.: On the dubins traveling salesman problem. IEEE Trans. Autom. Control **57**(1), 265–270 (2012)
10. Dubins, L.E.: On curves of minimal length with a constraint on average curvature, and with prescribed initial and terminal positions and tangents. Am. J. Math. **79**(3), 487–516 (1957)
11. Lee, J.H., Cheong, O., Kwon, W.C., Shin, S., Chwa, K.Y.: Approximation of curvature-constrained shortest paths

through a sequence of points. In: Paterson, M. (ed.) Algorithms - ESA 2000, Lecture Notes in Computer Science, vol. 1879, pp. 314–325. Springer, Berlin, Heidelberg (2000)
12. Ma, X., Castañón, D., et al.: Receding horizon planning for Dubins traveling salesman problems. In: Conference on Decision and Control, pp. 5453–5458. IEEE (2006)
13. Macharet, D., Campos, M.: An orientation assignment heuristic to the Dubins traveling salesman problem. In: Bazzan, A.L., Pichara, K. (eds.) Advances in Artificial Intelligence – IBERAMIA 2014, Lecture Notes in Computer Science, vol. 8864, pp. 457–468. Springer International Publishing (2014)
14. Macharet, D.G., Alves Neto, A., da Camara Neto, V.F., Campos, M.F.: Efficient target visiting path planning for multiple vehicles with bounded curvature. In: IEEE International Conference on Intelligent Robots and Systems (IROS), pp. 3830–3836 (2013)
15. Macharet, D.G., Neto, A.A., da Camara Neto, V.F., Campos, M.F.: Nonholonomic path planning optimization for Dubins' vehicles. In: IEEE International Conference on Robotics and Automation (Talk), pp. 4208–4213 (2011)
16. Macharet, D.G., Neto, A.A., da Camara Neto, V.F., Campos, M.F.: Data gathering tour optimization for Dubins' vehicles. In: Congress on Evolutionary Computation (CEC), pp. 1–8 (2012)
17. Manyam, S., Rathinam, S.: A tight lower bounding procedure for the dubins traveling salesman problem. Presented at the International Symposium on Mathematical Programming (2015). arXiv:1506.08752
18. Manyam, S., Rathinam, S., Casbeer, D.: Dubins paths through a sequence of points: lower and upper bounds. In: 2016 International Conference on Unmanned Aircraft Systems (ICUAS), pp. 284–291. IEEE (2016)
19. Manyam, S.G., Rathinam, S., Darbha, S.: Computation of lower bounds for a multiple depot, multiple vehicle routing problem with motion constraints. J. Dyn. Syst. Meas. Control. **137**(9), 094,501 (2015)
20. Manyam, S.G., Rathinam, S., Swaroop, D., Obermeyer, K.: Lower bounds for a vehicle routing problem with motion constraints. Int. J. Robot. Autom. **30**(3) (2015)
21. Manyam, S.G., Sivakumar R., Swaroop D.: Computation of lower bounds for a multiple depot, multiple vehicle routing problem with motion constraints. In: 52nd IEEE Conference on Decision and Control, Firenze, pp. 2378-2383 (2013)
22. Medeiros, A.C., Urrutia, S.: Discrete optimization methods to determine trajectories for dubins' vehicles. Electron Notes Discrete Math. **36**, 17–24 (2010). doi:10.1016/j.endm.2010.05.003. {ISCO} 2010 - International Symposium on Combinatorial Optimization. http://www.sciencedirect.com/science/article/pii/S1571065310000041
23. Oberlin, P., Rathinam, S., Darbha, S.: Today's traveling salesman problem. IEEE Robot. Autom. Mag. **17**(4), 70–77 (2010)
24. Pontryagin, L.S., Boltianski, V.G., Gamkrelidze, R.V., Mishchenko, E.F., Brown, D.E.: The Mathematical Theory of Optimal Processes. A Pergamon Press (1964). http://opac.inria.fr/record=b1122221
25. Rathinam, S., Sengupta, R., Darbha, S.: A resource allocation algorithm for multivehicle systems with nonholonomic constraints. IEEE Trans. Autom. Sci. Eng. **4**, 98–104 (2007). doi:10.1109/TASE.2006.872110
26. Rathinam, S., Pramod K.: An Approximation Algorithm for a Shortest Dubins Path Problem. arXiv:1604.05064 (2016)
27. Sadeghi, A., Smith, S.L.: On efficient computation of shortest dubins paths through three consecutive points. arXiv:1609.06662 (2016)
28. Sujit, P., Hudzietz, B., Saripalli, S.: Route planning for angle constrained terrain mapping using an unmanned aerial vehicle. J. Intell. Robot. Syst. **69**(1-4), 273–283 (2013)
29. Sussmann, H.J., Tang, G.: Shortest paths for the reeds-shepp car: a worked out example of the use of geometric techniques in nonlinear optimal control. Rutgers Center for Systems and Control Technical Report **10**, 1–71 (1991)
30. Tang, Z., Ozguner, U.: Motion planning for multitarget surveillance with mobile sensor agents. IEEE Trans. Robot. **21**(5), 898–908 (2005). doi:10.1109/TRO.2005.847567

Satyanarayana Gupta Manyam is NRC Research Associate at Air Force Research Laboratory, Wright-Patterson Air Force Base, OH. He received the Ph. D degree in Mechanical Engineering from Texas A & M University, College Station, TX in 2015. He also holds the M.S degree in Mechanical Engineering from State University of New York at Buffalo, Buffalo, NY, and the B.E degree in Mechanical Engineering from BITS, Pilani, India. His main research interests include cooperative routing of multi-vehicle systems, optimal path planning for autonomous vehicles, approximation algorithms and servo regulators for nonlinear systems.

Sivakumar Rathinam is currently an associate professor in mechanical engineering at the Texas A&M University, College Station. Prior to joining A&M, he was an associate research scientist at the University of California-NASA Ames Research Center. He received his Ph.D. degree in civil-systems engineering and M.S. in electrical engineering and computer science from the University of California in 2007 and 2006, respectively. His research interests include motion planning, combinatorial optimization, air traffic control and vision-based control.

David Wellman Casbeer received the B.S. and Ph.D. degrees in Electrical Engineering from Brigham Young University, Provo, UT, in 2003 and 2009, respectively. He was at the University of Sydney in 2007 as a visiting researcher studying distributed estimation and Gaussian processes. He is currently a Technical Area Lead (UAV Cooperative and Intelligence Control), in the Control Science Center of Excellence within the Air Force Research Laboratory with a focus on control and estimation for multiple UAVs under uncertainty. Dr. Casbeer is on the editorial board for the Journal of Intelligent & Robotic Systems. He is a Senior member of the IEEE and the AIAA. He is the chair for the AIAA Intelligent Systems Technical Committee.

Eloy Garcia received the Ph.D. degree from the Electrical Engineering Department, University of Notre Dame, Notre Dame, IN, in 2012. He also holds M.S. degrees from the University of Illinois at Chicago, Chicago, IL, and the University of Notre Dame, Notre Dame, IN, both in Electrical Engineering. Since 2012, Dr. Garcia has been a Research Scientist with Infoscitex Corporation, Dayton, OH, and with the Control Science Center of Excellence, Air Force Research Laboratory, Wright-Patterson Air Force Base, OH. His current research interests include cooperative control of multi-agent systems, differential games, and optimal and cooperative missile guidance.